Available online at www.sciencedirect.com
ScienceDirect
Bioorganic & Medicinal Chemistry Letters 16 (2006) 6281–6287
Bioorganic & Medicinal Chemistry Letters

Characterization of ATP-independent ERK inhibitors identified through in silico analysis of the active ERK2 structure

Fengming Chen,[a,†] Chad N. Hancock,[b,†] Alba T. Macias,[a] Joseph Joh,[a] Kimberly Still,[c] Shijun Zhong,[a] Alexander D. MacKerell, Jr.[a,*] and Paul Shapiro[a,*]

[a]*Department of Pharmaceutical Sciences, University of Maryland School of Pharmacy, Baltimore, MD 21201, USA*
[b]*Molecular and Cell Biology Program, University of Maryland, Baltimore, MD 21201, USA*
[c]*Senior Honors Program, Department of Biological Sciences, Villa Julie College, Stevenson, MD 21153, USA*

Received 3 July 2006; revised 4 September 2006; accepted 7 September 2006
Available online 26 September 2006

Abstract—The extracellular signal-regulated kinases (ERK1 and ERK2) are important mediators of cell proliferation. Constitutive activation of the ERK proteins plays a critical role in the proliferation of many human cancers. Taking advantage of recently identified substrate docking domains on ERK2, we have used computer-aided drug design (CADD) to identify novel low molecular weight compounds that interact with ERK2 in an ATP-independent manner and disrupt substrate-specific interactions. In the current study, a CADD screen of the 3D structure of active phosphorylated ERK2 protein was used to identify inhibitory compounds. We tested 13 compounds identified by the CADD screen in ERK-specific phosphorylation, cell proliferation, and binding assays. Of the 13 compounds tested, 4 compounds strongly inhibited ERK-mediated phosphorylation of ribosomal S6 kinase-1 (Rsk-1) and/or the transcription factor Elk-1 and inhibited the proliferation of HeLa cervical carcinoma cells with IC_{50} values in the 2–10 μM range. These studies demonstrate that CADD can be used to identify lead compounds for development of novel non-ATP-dependent inhibitors selective for active ERK and its interactions with substrates involved in cancer cell proliferation.

The mitogen activated protein (MAP) kinase family of enzymes regulates most biological processes including cell growth, proliferation, differentiation, inflammatory responses, and programmed cell death. Changes in MAP kinase activity have been implicated in the pathophysiology of cancer, inflammatory diseases, and neurodegenerative disorders.[1–4]

The three main members of MAP kinases include the extracellular signal-regulated kinases (ERK), the c-Jun N-terminal kinases (JNK), and p38 MAP kinases.[5] Currently, there is much interest in understanding the role of MAP kinases in disease as these proteins may be promising targets of new chemotherapy and anti-inflammatory agents.[6]

The ERK proteins consist of 2 isoforms (ERK1 and ERK2; referred to as ERK1/2) that are linked to the proliferation and survival of cancer cells.[7] The ERK1/2 pathway is commonly activated by extracellular ligands, which stimulate plasma membrane receptors and the sequential activation of Ras G-protein isoforms (H, K, and N-Ras), Raf isoforms (A, B, and C-Raf), and the MAP or ERK kinases-1 and 2 (MEK1/2), which are currently the only known activators of ERK1/2.[8] It is estimated that ERK1/2 can directly phosphorylate and regulate the activity of close to 70 different substrate proteins.[5,8] Many of the ERK1/2 substrates include other kinases, nuclear transcription factors, steroid hormone receptors, enzymes involved in generating signaling molecules, and structural proteins.[8] In the context of cancer cells, genetic mutations in membrane bound growth factor receptors, Ras, or Raf proteins can cause over-activation of the ERK1/2 pathway.[2,9,10] As such, much effort is being devoted to developing specific inhibitors of growth factor receptors, Ras, Raf, or MEK for new anti-cancer therapies. Several pharmacological inhibitors of Ras G-proteins, Raf kinases, and

Keywords: Extracellular signal-regulated kinase; Docking domains; Drug development; Computer-aided drug design.
* Corresponding authors. Tel.: +1 410 706 7442; fax: +1 410 706 0346 (A.D.M.); tel.: +1 410 706 8522 (P.S.); e-mail addresses: amackere@rx.umaryland.edu; pshapiro@rx.umaryland.edu
† These authors contributed equally to this paper.

0960-894X/$ - see front matter © 2006 Elsevier Ltd. All rights reserved.
doi:10.1016/j.bmcl.2006.09.038

MEK1/2 that have been developed are being tested in cancer clinical trials.[11–14]

ERK1/2 regulation of dozens of different proteins underscores the importance of these proteins in regulating a variety of cellular functions associated with normal and diseased tissue. Thus, we and others propose that selective ATP-independent inhibition of substrates involved in the disease processes, such as cancer cell proliferation, but not normal cell functions may be a more rationale approach for developing new chemotherapeutic agents.[15–17] The approach to selectively block ERK interactions with substrate proteins involves targeting specific docking domains that have been identified within the C-terminal lobe of MAP kinases.[18–21] The first ERK docking domains identified include the common docking (CD) and ED domains, which are located opposite the activation loop in the 3D crystallographic structure.[20] The CD and ED domains correspond to residues D316/D319 and T157/T158, respectively, in the rat ERK2 protein and these residues are conserved in the ERK1 isoform in both rodent and human species. In addition, other residues in the C-terminal regions of ERK proteins have been implicated to form docking sites involved in regulating the selectivity and specificity of substrate interactions.[18]

Our recent work has identified the first ATP-independent inhibitors of ERK1/2.[15] These findings used the 3D structure of unphosphorylated inactive ERK2 and computer-aided drug design (CADD) to identify low molecular weight compounds based on a structural groove between the CD and ED docking domain regions. Additional studies have demonstrated the feasibility of using CADD to identify low molecular weight inhibitors of protein–protein interactions.[22–25] As the activated ERK proteins are likely to be the more physiologically relevant target in the context of proliferating cancer cells, we extend the identification of lead compounds that disrupt ERK function using CADD applied to the 3D structure of the active phosphorylated ERK2 protein (Fig. 1). Out of 13 low molecular weight compounds identified by CADD and tested experimentally, we report the identification of four new compounds that inhibit ERK phosphorylation of substrate proteins.

The initial CADD in silico screening of active ERK2 identified many of the same compounds that were identified using the unphosphorylated ERK2 structure suggesting that conformational changes occurring in ERK2 upon phosphorylation are minimal in this region of the protein.[44] Comparison of the conformations of the two forms of the protein from crystallographic studies[26,27] shows both the overall structures (Fig. 1A) as well as the regions in the vicinity of the CD and ED domains to be similar (Fig. 1B). The considerable overlap is consistent with the reported lack of a conformational change in the ED region of active ERK as measured by changes in deuterium exchange.[45] However, some changes in deuterium exchange rates within the region containing the CD domain have been observed.[45] Such differences, which may be due to either subtle differences in structure or changes in the flexibility of the protein, indicate that targeting active ERK2 may identify additional ERK docking domain inhibitors. As such, 45 new compounds were identified by CADD screening the 3D structure of phosphorylated ERK2. The molecular weights of compounds identified using active ERK2 ranged from 188 to 486 amu with an average and standard deviation of 388 ± 68 amu. The 13 compounds that were identified from the Chembridge chemical library were purchased and tested further in biological assays.

The new compounds were first tested for inhibition of ERK-mediated phosphorylation of the transcription factor Elk-1, which is an important regulator of cell proliferation.[46] Cells were treated with EGF to activate the ERK pathway and phosphorylation of Elk-1 on the ERK site at S383 was detected by immunoblot analysis (Fig. 2A). The test compounds inhibited Elk-1 phosphorylation by 20–100% compared to the EGF control (Fig. 2A). Compounds **89**, **92**, **93**, and **95** were most effective at inhibiting Elk-1 phosphorylation at 100 μM (Fig. 2A). The effects of the test compounds were also

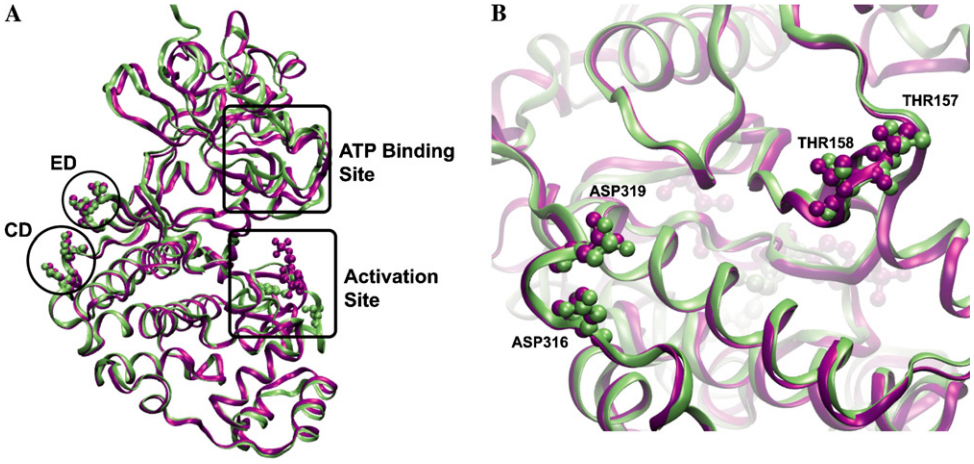

Figure 1. Superimposed structures of the unphosphorylated (green) and phosphorylated (purple) forms of ERK2. (A) Superimposed ribbon image showing the location and conformational changes associated with the ATP-binding domain, activation site, and the ED and CD domains. (B) Superimposed ribbon image in the vicinity of the CD (Asp 316 and 319) and ED (Thr 157 and 158) domains.

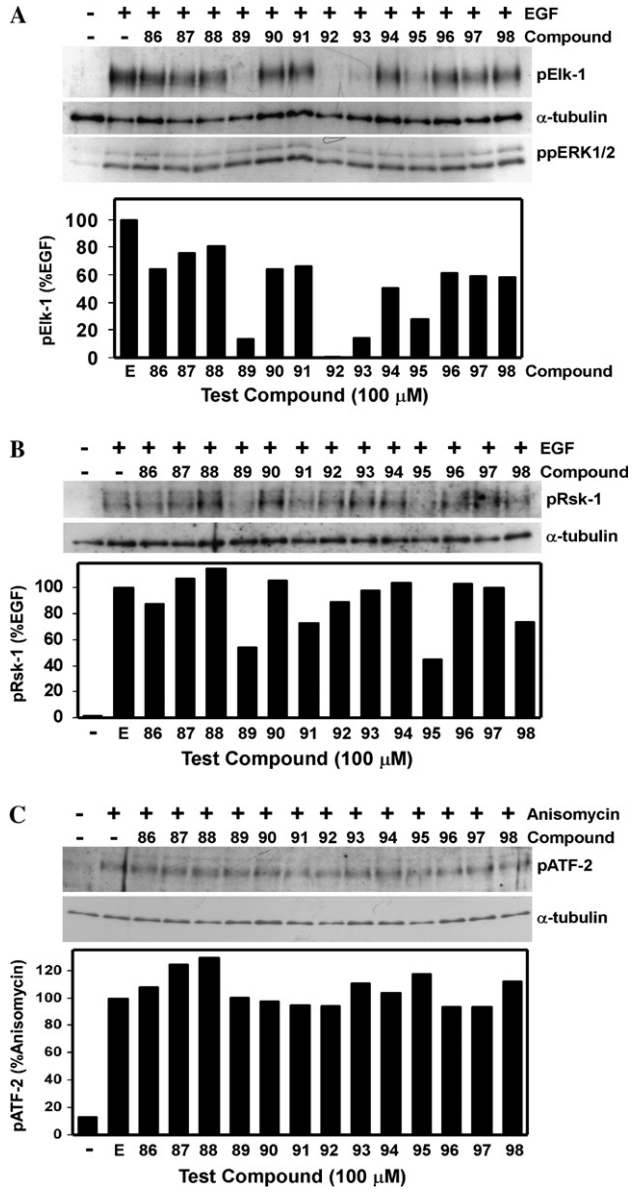

Figure 2. Effects of test compounds on ERK substrate phosphorylation. HeLa cells were pre-treated with or without 100 μM of the test compounds listed for 15 min prior to the addition of epidermal growth factor (EGF or E) to stimulate the ERK pathway or anisomycin (A) to stimulate p38 MAP kinase. Cells were harvested and the extracted proteins were subjected to immunoblot analysis. (A) Immunoblots of Elk-1 phosphorylated on S383 (pElk-1), α-tubulin, and active ERK1/2 (ppERK1/2). The lower graph shows the quantification of the ratio of pElk-1 to α-tubulin as measured by densitometry. The pElk-1 phosphorylation in the presence of the test compounds was compared to the EGF only treatment, which was set at 100%. (B) Immunoblots of Rsk-1 phosphorylated on T573 (pRsk-1) and α-tubulin as a loading control. The lower graph shows the quantification of the ratio of pRsk-1 to α-tubulin as measured by densitometry. The pRsk-1 phosphorylation in the presence of the test compounds was compared to the EGF only treatment, which was set at 100%. (C) Immunoblot analysis of phosphorylated ATF2 (pATF2) and α-tubulin as a loading control. The lower graph shows the quantification of the ratio pATF2 to α-tubulin as measured by densitometry. The pATF2 phosphorylation in the presence of the test compounds was compared to the anisomycin (A) only treatment, which was set at 100%. The data were reproduced in at least three independent experiments.

tested with Rsk-1, another ERK substrate involved in regulating cell proliferation. Compounds **89**, **91**, and **95** were the most effective at inhibiting ERK-mediated Rsk-1 phosphorylation (Fig. 2B).

It is not surprising that different test compounds have different effects on these two ERK substrates. While the inhibition of Rsk-1 can be explained by the test compounds designed to bind to the CD region, which is required for Rsk-1 interactions with ERK2, it is not entirely apparent why the test compounds would interfere with Elk-1 interactions, which are thought to use different ERK residues for interactions.[16] It is possible that the test compounds bind to other regions of ERK proteins or that the test compounds have allosteric effects. Importantly, such differential inhibitory specificity of the inhibitors indicates that the identification substrate-specific inhibitors of ERK are feasible. Future studies are aimed at characterizing the interactions between the active test compounds and ERK proteins.

The test compounds were also tested for selectivity for ERK versus the p38 MAP kinase. The phosphorylation of ATF2, a transcription factor substrate for the p38 MAP kinase, was not affected by any of the test compounds (Fig. 2C). In addition, the test compounds did not affect ERK1 and ERK2 phosphorylation, indicating that they do not inhibit the upstream ERK activating proteins, MEK1 or MEK2 (Fig. 2A). Thus, the active compounds appear to show selectivity toward ERK. The structures of the 13 compounds tested are shown in Figure 3.

The effects of the test compounds on cell proliferation were tested using a colony formation assay.[47] In these assays, HeLa cells are plated at a low density in the presence or absence of the test compounds. After 8–10 days incubation the number of cell colonies that form were stained and quantified under each condition. Test compounds **86** and **89** were the most effective inhibitors of cell proliferation with IC_{50} values of 5 μM or less (Table 1). Test compounds **93**, **94**, and **95** were also effective inhibitors of cell proliferation with IC_{50} values in the 5–10, 25–50, and 10–25 μM range, respectively. Although test compound **92** was a potent inhibitor of Elk-1 phosphorylation, the IC_{50} in the growth assay was approximately 75 μM (Table 1). Test compound **89** was the most effective in inhibiting both Elk-1 and Rsk-1 phosphorylation and cell proliferation (Fig. 2 and Table 1). These findings indicate that compound **89** may be a useful lead for further development as an anti-cancer agent. Future studies are aimed at further characterization of the ERK substrates affected by these compounds.

Lastly, fluorescence spectroscopy experiments were used as a preliminary determination of whether the active compounds interact with the ERK2 protein.[48] Fluorescence quenching of ERK2 by the test compounds is indicative of binding interactions and potential protein conformational changes. Compounds **92** and **95** were effective in quenching ERK2 fluorescence with K_D values of approximately 45 and 16 μM, respectively

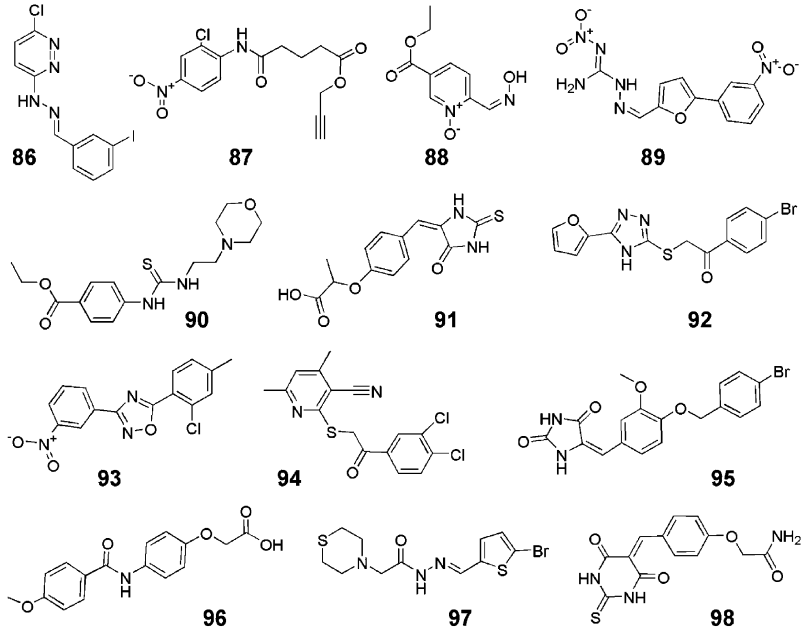

Figure 3. Chemical structures of the thirteen compounds tested in this study.

Table 1. Effects of test compounds on cell proliferation

Compound	IC_{50} (μM)
86	~5
87	>100
88	>100
89	<2
90	>100
91	>100
92	~75
93	5–10
94	25–50
95	10–25
96	>100
97	>100
98	>100

HeLa cells were plated at low density and incubated with a single dose (0–100 μM) of the test compounds being tested. After 8–10 days, the resulting cell colonies were stained, photographed, and counted to estimate the IC_{50}. The data is derived from at least three independent experiments.

(Fig. 4A). Compound **93**, which caused some quenching of ERK2 fluorescence, underwent auto-fluorescence at higher concentrations (Fig. 4A). The lack of fluorescence quenching by compound **94** suggested that this molecule did not bind ERK2 and that its effects on substrate phosphorylation and cell proliferation were potentially non-specific. Additional test compounds, including **89** and **98**, also caused fluorescence quenching indicative of interactions with ERK2 with an approximate K_D of 13 and 20 μM, respectively (Fig. 4B). Although compound **86** also caused some fluorescence quenching at concentrations of 20 μM or less, this compound became insoluble at concentrations of 50 μM or higher and was therefore not analyzed further.

The findings in this study extend our identification of novel compounds that may be used as substrate selective ERK inhibitors. Using the 3D structure of active ERK2, CADD 45 new compounds with the potential for interacting with the regions around CD and ED docking domains. These new compounds were not previously identified using the non-active ERK2 3D structure.[15] Of these, 13 molecules were tested in this study with two of the compounds (**89** and **95**) interfering with the phosphorylation of ERK substrates, inhibiting cell proliferation, and binding with purified

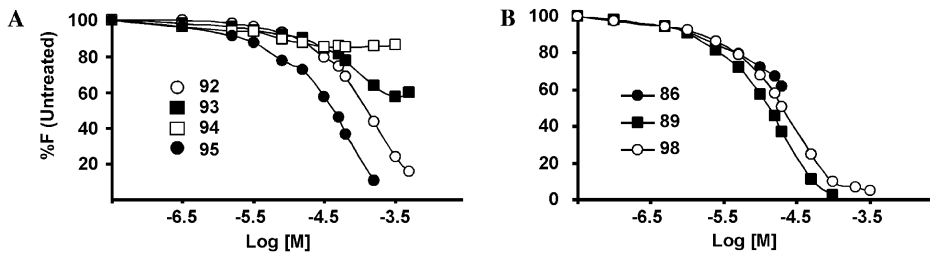

Figure 4. Effects of test compounds on ERK2 fluorescence. (A) Fluorescence titrations were done with test compounds **92** (open circles), **93** (closed squares), **94** (open squares), and **95** (closed circles). (B) Fluorescence titrations with test compounds **86** (closed circles), **89** (closed squares), and **98** (open circles). The percentage of ERK2 fluorescence (*F*) was plotted against the log concentration in mol/l (Log [*M*]) of each test compound using the peak fluorescence in the absence of test compound set at 100% as the reference.

ERK2 protein as determined via fluorescence quenching. Three other compounds (**86**, **93**, and **94**) inhibited cell proliferation but were less effective at binding to purified ERK2. In addition, compound **98**, which binds ERK2 and partially inhibits substrate phosphorylation, had no effect on cell proliferation. Importantly, none of the test compounds had any effect on the phosphorylation of ATF2, a specific substrate for p38 MAP kinases. The varying effects on ERK signaling by 6 of the 13 test compounds warrant further testing and development of these molecules as substrate-specific ERK inhibitors. That the active compounds identified were from such a small pool of starting molecules provides further evidence for the advantages of using in silico pre-screening in order to save time and expenses involved in doing biological assays with large chemical libraries.

Acknowledgments

This work was supported by grants from the National Institutes of Health (CA105299-01 to P.S., CA95200-01 to A.D.M., and CA095200-03S1 to A.T.M.) and by the University of Maryland, Baltimore Computer-Aided Drug Design Center.

References and notes

1. Kyriakis, J. M.; Avruch, J. *BioEssays* **1996**, *18*, 567.
2. Reuter, C. W.; Morgan, M. A.; Bergmann, L. *Blood* **2000**, *96*, 1655.
3. Duesbery, N. S.; Webb, C. P.; Vande Woude, G. F. *Nat. Med.* **1999**, *5*, 736.
4. Shapiro, P. *Crit. Rev. Clin. Lab. Sci.* **2002**, *39*, 285.
5. Pearson, G.; Robinson, F.; Beers Gibson, T.; Xu, B. E.; Karandikar, M.; Berman, K.; Cobb, M. H. *Endocr. Rev.* **2001**, *22*, 153.
6. Cohen, P. *Curr. Opin. Chem. Biol.* **1999**, *3*, 459.
7. Kohno, M.; Pouyssegur, J. *Prog. Cell Cycle Res.* **2003**, *5*, 219.
8. Lewis, T. S.; Shapiro, P. S.; Ahn, N. G. *Adv. Cancer Res.* **1998**, *74*, 49.
9. Bos, J. L. *Cancer Res.* **1989**, *49*, 4682.
10. Brose, M. S.; Volpe, P.; Feldman, M.; Kumar, M.; Rishi, I.; Gerrero, R.; Einhorn, E.; Herlyn, M.; Minna, J.; Nicholson, A.; Roth, J. A.; Albelda, S. M.; Davies, H.; Cox, C.; Brignell, G.; Stephens, P.; Futreal, P. A.; Wooster, R.; Stratton, M. R.; Weber, B. L. *Cancer Res.* **2002**, *62*, 6997.
11. Bollag, G.; Freeman, S.; Lyons, J. F.; Post, L. E. *Curr. Opin. Investig. Drugs* **2003**, *4*, 1436.
12. Boldt, S.; Kolch, W. *Curr. Pharm. Des.* **2004**, *10*, 1885.
13. Sebolt-Leopold, J. S. *Curr. Pharm. Des.* **2004**, *10*, 1907.
14. Allen, L. F.; Sebolt-Leopold, J.; Meyer, M. B. *Semin. Oncol.* **2003**, *30*, 105.
15. Hancock, C. N.; Macias, A.; Lee, E. K.; Yu, S. Y.; Mackerell, A. D., Jr.; Shapiro, P. *J. Med. Chem.* **2005**, *48*, 4586.
16. Dimitri, C. A.; Dowdle, W.; MacKeigan, J. P.; Blenis, J.; Murphy, L. O. *Curr. Biol.* **2005**, *15*, 1319.
17. Hancock, C. N.; Macias, A. T.; Mackerell, A. D., Jr.; Shapiro, P. *Med. Chem.* **2006**, *2*, 213.
18. Zhang, J.; Zhou, B.; Zheng, C. F.; Zhang, Z. Y. *J. Biol. Chem.* **2003**, *278*, 29901.
19. Nichols, A.; Camps, M.; Gillieron, C.; Chabert, C.; Brunet, A.; Wilsbacher, J.; Cobb, M.; Pouyssegur, J.; Shaw, J. P.; Arkinstall, S. *J. Biol. Chem.* **2000**, *275*, 24613.
20. Tanoue, T.; Adachi, M.; Moriguchi, T.; Nishida, E. *Nat. Cell. Biol.* **2000**, *2*, 110.
21. Liu, S.; Sun, J. P.; Zhou, B.; Zhang, Z. Y. *Proc. Natl. Acad. Sci. U.S.A.* **2006**, *103*, 5326.
22. Markowitz, J.; Chen, I.; Gitti, R.; Baldisseri, D. M.; Pan, Y.; Udan, R.; Carrier, F.; MacKerell, A. D., Jr.; Weber, D. J. *J. Med. Chem.* **2004**, *47*, 5085.
23. Loughney, D. A.; Murray, W. V.; Jolliffe, L. K. *Med. Chem. Res.* **1999**, *9*, 579.
24. Zeng, J.; Nheu, T.; Zorzet, A.; Catimel, B.; Nice, E.; Maruta, H.; Burgess, A. W.; Treutlein, H. R. *Protein Eng.* **2001**, *14*, 39.
25. Huang, N.; Nagarsekar, A.; Xia, G.; Hayashi, J.; MacKerell, A. D., Jr. *J. Med. Chem.* **2004**, *47*, 3502.
26. Zhang, F.; Strand, A.; Robbins, D.; Cobb, M. H.; Goldsmith, E. J. *Nature* **1994**, *367*, 704.
27. Canagarajah, B. J.; Khokhlatchev, A.; Cobb, M. H.; Goldsmith, E. J. *Cell* **1997**, *90*, 859.
28. Bernstein, F. C.; Koetzle, T. F.; Williams, G. J.; Meyer, E. F., Jr.; Brice, M. D.; Rodgers, J. R.; Kennard, O.; Shimanouchi, T.; Tasumi, M. *Eur. J. Biochem.* **1977**, *80*, 319.
29. Kuntz, I. D.; Blaney, J. M.; Oatley, S. J.; Langridge, R.; Ferrin, T. E. *J. Mol. Biol.* **1982**, *161*, 269.
30. Kuntz, I. D. *Science* **1992**, *257*, 1078.
31. Connolly, M. L. *Science* **1983**, *221*, 709.
32. Ferrin, T. E.; Huang, C. C.; Jarvis, L. E.; Langridge, R. *J. Mol. Graph.* **1988**, *6*, 13.
33. Tanoue, T.; Maeda, R.; Adachi, M.; Nishida, E. *EMBO J.* **2001**, *20*, 466.
34. Goodford, P. J. *J. Med. Chem.* **1984**, *28*, 849.
35. Pan, Y.; Huang, N.; Cho, S.; MacKerell, A. D., Jr. *J. Chem. Inf. Comput. Sci.* **2003**, *43*, 267.
36. Leach, A. R.; Kuntz, I. D. *J. Comput. Chem.* **1992**, *13*, 730.
37. Ewing, T. J. A.; Kuntz, I. D. *J. Comput. Chem.* **1997**, *18*, 1175.
38. Butina, D. *J. Chem. Inf. Comp. Sci.* **1999**, *39*, 747.
39. Lipinski, C. A.; Lombardo, F.; Dominy, B. W.; Feeney, P. J. *Adv. Drug. Deliv. Rev.* **2001**, *46*, 3.
40. Cha, H.; Lee, E. K.; Shapiro, P. *J. Biol. Chem.* **2001**, *276*, 48494.
41. Dangi, S.; Cha, H.; Shapiro, P. *Cell Signal.* **2003**, *15*, 667.
42. Cha, H.; Hancock, C.; Dangi, S.; Maiguel, D.; Carrier, F.; Shapiro, P. *Biochem. J.* **2004**, *378*, 857.
43. Shapiro, P. S.; Whalen, A. M.; Tolwinski, N. S.; Wilsbacher, J.; Froelich-Ammon, S. J.; Garcia, M.; Osheroff, N.; Ahn, N. G. *Mol. Cell. Biol.* **1999**, *19*, 3551.
44. The CADD screening approach using the 3D structure of ERK2 in the unphosphorylated state has been previously described.[15] In the current studies, the 3D structure of ERK2 in the phosphorylated state[26,27] was retrieved from the Protein DataBank, deposition number 1ERK.[28] Charges and hydrogens were added using SYBYL6.4 (Tripos, Inc.). All docking calculations were carried out with DOCK[29] using flexible ligands based on the anchored search method.[30] The solvent accessible surface[31] was calculated with the program DMS[32] using a surface density of 2.76 surface points per $Å^2$ and a probe radius of 1.4 $Å^2$. Sphere sets were calculated with the DOCK associated program SPHGEN. From the full sphere set, sphere clusters in the ERK2 docking domains important for interactions with the protein substrates were identified. Based on mutagenesis experiments, residues involved in intermolecular interactions were used to select the docking site. These include D316 and D319 in the C-terminus,[20]

which are part of the common docking (CD) domain, and residues T157 and T158, which contribute to the ED docking domain.[33] Spheres within both 10 Å of the CD domain and 12 Å of the ED domains were selected. The resulting sphere set contained 11 spheres and was located in the groove between the CD and ED domains as described.[15] The selected sphere set acted as the basis for initial ligand placement during database searching. The GRID method[34] within DOCK was used to approximate the ligand–receptor interaction energy during ligand placement by the sum of the electrostatic and van der Waals (vdW) components. Interaction energies, IE, were normalized via $IE_{norm} = IE/Nx$, where N is the number of non-hydrogen atoms in a ligand and x is a factor empirically selected to correct for the bias of IE-based scoring methods to favor large molecular-weight compounds, as previously described.[35] The GRID box dimensions were $25.3 \times 26.6 \times 27.3$ Å^3 centered around the sphere set to ensure that docked molecules were within the grid. Database screening targeted the set of 20,000 compounds previously chosen from method 1 docking of 800,000 compounds against the unphosphorylated, inactive form of ERK.[15] Docking applied the more rigorous secondary docking procedure applied in the previous study with the only difference being the use of the phosphorylated ERK2 3D structure. Docking was performed by dividing each compound into non-overlapping rigid segments connected by rotatable bonds. Segments with more than 5 heavy atoms were used as anchors, each of which was docked into the binding site in 250 orientations and minimized. The remainder of the molecule was built around the anchor in a stepwise fashion by adding other segments connected through rotatable bonds. At each step, the dihedral of the rotatable bond was sampled in increments of 10° and the lowest energy conformation was selected. All rotatable bonds were minimized simultaneously during the stepwise building of the molecule. Pruning of the conformations ensured conformational diversity and more favorable energies.[36,37] Energy scoring was performed with a distant-dependent dielectric, with a dielectric constant of 4, and using an all atom model. The total interaction energies for the best orientation of each were then normalized using $x = 0$, 0.33, 0.5, 0.67, and 1.0 yielding five sets of 500 compounds from each normalization. Based on analysis of the molecular weight distributions of the five sets the $x = 0$ and $x = 0.33$ sets, with average molecular weights of 264 and 255 amu, respectively, were selected and the two sets combined. This yielded a set of approximately 700 unique compounds for similarity clustering after removing those compounds common to both sets. Chemical similarity clustering of the ~700 unique compounds was performed to maximize the chemical diversity of the final compounds selected for biological assay. Clustering calculations were performed using the program MOE (Chemical Computing Group, Inc.). The Jarvis–Patrick algorithm, as implemented in MOE, was used to cluster the compounds using the MACC_BITS fingerprinting scheme and Tanimoto coefficient (TC). It first calculates the MACC_BITS fingerprints which encode the 2D structural features for each compound into linear bit strings of data. The pairwise similarity matrix between each compound was calculated based on the TC values.[38] TC is one of the metrics available that provides a similarity score by dividing the fraction of features common to both molecules by the total number of features. The similarity matrix is then converted into a second matrix in which each TC value is replaced by a 0 or 1 representing similarity values below and above the threshold value (S) provided by the user, respectively. The rows of the new matrix are treated as fingerprints and the 'TC' value between each is calculated. Molecules with values above the selected overlap threshold (T) are put in the same cluster. A 70–40 similarity/overlap value was used to cluster the compounds. Compounds for experimental assay were chosen from the individual clusters with emphasis on compounds with drug-like physical characteristics as defined by Lipinski et al.[39] Properties considered were the MW, number of hydrogen donors (NHD) and acceptors (NHA), and the log P values as calculated by MOE. However, exceptions were made when all compounds in a cluster had one or more physical characteristics beyond the range defined by Lipinski et al.[39] In addition, only those compounds that were not previously studied[15] were selected with a majority of those compounds selected from clusters in which there were no compounds that had been previously tested. Of the total of 45 compounds selected via CADD those available from ChemBridge (San Diego, CA, 13 compounds total) were purchased and dissolved in DMSO at a stock concentration of 25 mM. The identity of the test compounds was verified by mass spectrometry.

45. Hoofnagle, A. N.; Resing, K. A.; Goldsmith, E. J.; Ahn, N. G. *Proc. Natl. Acad. Sci. U.S.A.* **2001**, *98*, 956.
46. HeLa (human cervical carcinoma) cells were purchased from American Type Culture Collection (ATCC, Manassas, VA). HeLa cells were cultured in a complete medium consisting of Dulbecco's modified Eagle's medium (DMEM) supplemented with 10% fetal bovine serum (FBS) and antibiotics (Penicillin, 100 U/ml; Streptomycin, 100 μg/ml) (Invitrogen, Carlsbad, CA). Epidermal growth factor (EGF) was purchased from Sigma (St. Louis, MO) and used at 25 ng/ml final concentration. Antibodies against phosphorylated Rsk-1 (pT573), Elk-1 (pS383), ATF-2 (pT71), and ERK (pT183, pY185) were purchased from Cell Signaling Technologies (Woburn, MA), Santa Cruz Biotech (Santa Cruz, CA), or Sigma. The α-tubulin antibody was purchased from Sigma. Prior to harvesting, cells were pre-incubated with the test compounds for 15–20 min and then stimulated with EGF or anisomycin to activate the ERK or p38 MAP kinase pathways, respectively. Control and treated cells were washed twice with cold phosphate-buffered saline (PBS, pH 7.2; Invitrogen) and proteins were collected following cell lysis with SDS–PAGE loading buffer. The protein lysates were then separated on SDS–PAGE for immunoblot analysis, which was done as previously described.[40–43]
47. Trypsinized cells were plated on 12- or 24-well plates at low densities (200–400 cells per well) in the absence (DMSO only) or presence of test compounds. In additional experiments, cells were first allowed to adhere to the culture dishes for 16 h prior to treatment with test compounds. The treated cells received a single dose of the test compounds at the beginning of the experiments. The control and treated cells were grown for 8–14 days to allow the formation of colonies. Cells were then fixed for 10 min in 4% paraformaldehyde and stained with 0.2% crystal violet in 20% methanol for 1–2 min. Following several washes with distilled water, the colonies (containing at least 40 cells) were counted. Each individual experiment was repeated on at least three separate occasions.
48. $(His)_{X6}$-tagged ERK2 was bacterially expressed and the cells harvested in BugBuster protein extraction reagent (EMD Biosciences, San Diego, CA). Clarified lysates were loaded onto a Talon Co^{2+}-IMAC affinity chromatography resin column (BD Biosciences, San Jose, CA), and the bound protein eluted using increasing concentrations of

imidazole. SDS–PAGE electrophoresis and Coomassie blue staining were used to identify the eluted fractions containing the ERK2 protein. The ERK2 protein concentration was determined using Bradford Reagent (Sigma). Fluorescence spectra were recorded with a Luminescence Spectrometer LS50 (Perkin-Elmer, Boston, MA). For all experiments, ERK2 protein was diluted into 20 mM Tris–HCl, pH 7.5. Titrations were performed by increasing the test compound concentration while maintaining the ERK2 protein concentration at 3 μM. The excitation wavelength was 295 nm and fluorescence was monitored from 300 to 500 nm. All reported fluorescence intensities are relative values and are not corrected for wavelength variations in detector response. Dissociation constants, K_D, were determined using reciprocal plots, $1/v$ vs $1/[I]$, where v represents the percent occupied sites calculated assuming fluorescence quenching to be directly proportion to the percentage of occupied binding sites, $[I]$ represents the concentration of the inhibitor compound, and the slope of the curve equals the K_D.